Available online at www.sciencedirect.com
SCIENCE DIRECT®
Phytochemistry 66 (2005) 323–335
PHYTOCHEMISTRY
www.elsevier.com/locate/phytochem

Metabolic flux analysis in complex isotopolog space. Recycling of glucose in tobacco plants

Christian Ettenhuber [a], Tanja Radykewicz [a], Waltraud Kofer [b], Hans-Ulrich Koop [b], Adelbert Bacher [a], Wolfgang Eisenreich [a,*]

[a] *Lehrstuhl für Organische Chemie und Biochemie, Technische Universität München, Lichtenbergstr. 4, D-85747 Garching, Germany*
[b] *Bereich Botanik, Department I, Fakultät für Biologie, Ludwigs-Maximilians-Universität München, Menzinger Str. 67, D-80638 München, Germany*

Received 24 June 2004; received in revised form 8 December 2004

Abstract

Tobacco plants grown in vitro were supplied with a mixture of [U-$^{13}C_6$]glucose and unlabelled sucrose via the root system. After 20 days, leaves were harvested and extracted with water. Glucose was isolated from the extract and was analysed by ^{13}C NMR spectroscopy. All ^{13}C signals appeared as complex multiplets due to ^{13}C–^{13}C coupling. The abundance of 21 isotopologous glucose species was determined from the ^{13}C NMR signal integrals by numerical deconvolution using a genetic algorithm. The relative fractions of specific isotopologs in the overall excess of ^{13}C-labelled specimens establish flux contributions via glycolysis/glucogenesis, pentose phosphate pathway, citric acid cycle and Calvin cycle including $^{13}CO_2$ refixation. The fluxes were modelled and reconstructed in silico by a novel rule-based approach yielding the contributions of circular pathways and the degree of multiple cycling events. The data indicate that the vast majority of the proffered [U-$^{13}C_6$]glucose molecules had been modified by catabolism and subsequent glucogenesis from catabolic fragments, predominantly via passage through the citric acid cycle and the pentose phosphate pathway.

Keywords: *Nicotiana tabacum*; Metabolism; Carbon flux; NMR; Isotopolog; In silico modelling

1. Introduction

The past decade has provided an unprecedented and essentially unexpected wealth of genomic data via whole genome sequencing. One of the surprises was the finding that the genetic complexity of higher plants is similar, if not superior to that of animals. More specifically, the comparison between the mouse and human genome suggested that mammals in general have about 25,000 genes (International Human Genome Sequencing Consortium, 2004). The draft sequence of *Arabidopsis thaliana* suggested about 25,000 genes (Arabidopsis Genome Initiative, 2001; Yamada et al., 2003), and the draft sequence of rice suggested approximately 60,000 genes (Goff et al., 2002). More recently, the finished sequence of rice chromosome 10 which accounts for about 5% of the total genome was shown to comprise about 3400 genes (Rice Chromosome 10 Sequencing Consortium, 2003).

Whereas these findings are not understood in detail, it appears safe to assume that the unexpected complexity of plant genomes reflects in part the extraordinary complexity of plant metabolism. Approximately 9000 *A. thaliana* genes have been estimated to code for enzymes.

The overall complexity of metabolic networks can be estimated to vary between many dozens of nodes (in

* Corresponding author. Tel.: +49 89 289 13336; fax: +49 89 289 13363.
E-mail address: wolfgang.eisenreich@ch.tum.de (W. Eisenreich).

0031-9422/$ - see front matter © 2004 Elsevier Ltd. All rights reserved.
doi:10.1016/j.phytochem.2004.12.014

case of the simplest known bacteria, especially *Mycoplasma*, cf. Fraser et al., 1995) to many thousands of nodes in higher plants (a node in the metabolic networks being defined as a metabolite which can be generated and/or consumed by one or several different metabolic routes). Despite the complexity of these networks, the connections between different nodes tend to be short. Metabolic networks have the character of so-called "small world networks" (Clifton and Roe, 1998; Bray, 2003).

A more detailed understanding of the complex metabolic networks of crop plants is believed to be one of the prerequisites for rapid progress in agricultural yields which appears indispensable in order to feed the rapidly growing human population. A wide variety of techniques have become available for this purpose. Thus, the biosynthesis of proteins involved in metabolism can be addressed by RNA profiling and by advanced methods of proteomic analysis (Fey et al., 1997; Eisenberg et al., 2000; Lockhart and Winzeler, 2000). The overall performance of multienzyme systems can then be addressed by numerical simulation methods (with the caveat that the catalytic signatures of individual enzymes are typically not accurate enough for this type of analysis). Alternatively, profiles describing the concentrations of numerous metabolites can be obtained by rapidly progressing mass spectroscopic technology (Brunengraber et al., 1997; Fiehn et al., 2000).

The quantitative analysis of metabolite flux in complex metabolic networks can be achieved by isotopolog perturbation/relaxation methods (Eisenreich et al., 1993, 2004; Szyperski, 1995; Bacher et al., 1999; Glawischnig et al., 2002; Kruger et al., 2003). Briefly, organic matter is composed of all stable isotopes of elements such as hydrogen, carbon, nitrogen, oxygen and sulphur. Specifically, the isotopes ^{12}C and ^{13}C account for 98.9% and 1.1%, respectively, of naturally occurring elemental carbon. In natural organic matter, the distribution of the two carbon isotopes follows an almost random pattern. Small deviations from random distribution are caused by geophysical and biological processes (Rossmann et al., 1991; Schmidt, 2003) and can be used for a wide variety of diagnostic approaches (Gleixner et al., 1993; Müller et al., 2003) but are well below the sensitivity level of the perturbation/relaxation methodology used in this paper.

The near-equilibrium distribution of ^{13}C can be perturbed by the introduction of any ^{13}C-labelled feed supplement(s) into any metabolic system. The perturbation will then spread in the metabolic network by way of enzyme-catalysed reactions, ultimately through virtually every part of the network. In light of the "small world" character of metabolic networks (Bray, 2003) that spreading process can occur rapidly. The relaxation process can be probed by analysis of the ^{13}C abundance at different nodes in the network (i.e., by analysis of the isotope composition of different metabolites) using mass spectrometry or NMR spectroscopy.

Glucose phosphate can be considered as one of the central nodes in metabolic networks. Any stable carbon atom in a given glucose molecule can be either ^{12}C or ^{13}C. Hence, $2^6 = 64$ isotopologous species must be taken into account for a comprehensive description of the six carbon compound glucose. In naturally occurring glucose, approximately 93 mol% are present as [U-$^{12}C_6$]glucose, and approximately 7 mol% of glucose molecules carry a single ^{13}C atom in any of the six possible positions. On stochastic grounds, multiply ^{13}C-labelled molecular species are rare (since the natural abundance of ^{13}C is only about 1.1%). For example, the abundance of [U-$^{13}C_6$]glucose in the naturally occurring carbohydrate is about 10^{-10} mol%. The introduction of exogenous [U-$^{13}C_6$]glucose can increase the relative abundance of that particular isotopolog by more than 10 orders of magnitude.

In this paper, we have analysed the fate of ^{13}C-labelled glucose fed to intact tobacco plants via the root system. The analysis of glucose isolated from the leaves of these plants showed that the vast majority of glucose molecules had a complex history of disassembly and reassembly. A rule-based computational simulation of the isotopolog composition reveals the catabolism of glucose and the regeneration of glucose from components of the complex metabolite pool in considerable detail.

2. Results

In tobacco, the isotope distribution of glucose can be easily perturbed by feeding a ^{13}C-labelled glucose isotopolog to intact plants via the root system. In the present study, a mixture of 2% [U-$^{13}C_6$]glucose and 98% unlabelled sucrose with natural ^{13}C distribution (1.1% overall ^{13}C abundance) was added to the solid agar support on which the plants were grown under aseptic conditions. After a growth period of 20 days, the plants were harvested, the leaves were pulverised under liquid nitrogen, and the powder was extracted with water. Glucose was isolated chromatographically from the extract and was analysed by ^{1}H and ^{13}C NMR spectroscopy.

The ^{1}H NMR signal for H-1α (=5.14 ppm) shows satellite pairs caused by ^{1}H–^{13}C-coupling ($^{1}J_{CH}$ = 170 Hz) (Fig. 1). The absolute ^{13}C abundance of C-1α can be calculated via the intensities of these ^{13}C-coupled satellites and equals 2.4% (corresponding to a ^{13}C excess of 1.3 mol%). This value is used as the reference for the other carbon atoms in glucose.

The ^{13}C signals of the isolated glucose appear as complex multiplets as a consequence of ^{13}C–^{13}C coupling

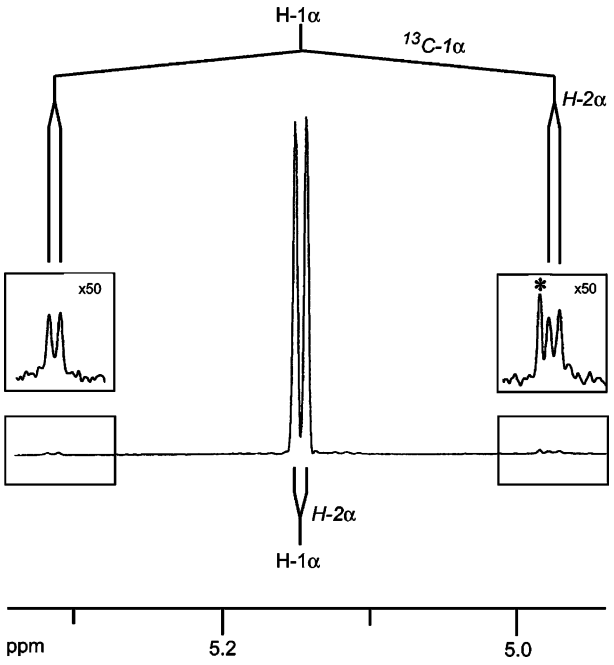

Fig. 1. ^{1}H NMR signal of H-1α of glucose from tobacco in the experiment with [U-$^{13}C_6$]glucose. Signals arising by coupling with ^{13}C-1 are indicated; the asterisk indicates a signal of a contaminant.

(Fig. 2). The ^{13}C spectrum is additionally complicated by the simultaneous presence of the α and β anomers of glucose in a state of chemical equilibrium. However, this additional layer of complexity is in fact a blessing in disguise because it can be utilised in order to check the accuracy of the quantitative data.

The ^{13}C signal of C-1 of the α anomer can serve to illustrate the method (Fig. 3). The central line indicated by A in the figure is characteristic for glucose molecules in the α anomer form which carry ^{13}C in position 1 and ^{12}C in position 2, irrespective of the labelling pattern in carbons 3–6. The satellite signals indicated by B arise by coupling between ^{13}C in position 1 and a second ^{13}C atom in position 2. The long-range couplings reflected by the broadened line in the satellite pairs (Fig. 3(a)) can be resolved by appropriate data processing (i.e., by applying a "strong" Gaussian function to the signal of the free induction decay (FID) prior to Fourier transformation) as shown in Fig. 3(b). Based on published coupling constants and isotope shifts (Eisenreich et al., 2004), these satellites document the presence of ^{13}C at positions 5 and 6 (Fig. 3(b)).

A quantitative description of the isotopolog population can be extracted, in principle, from the ratio between the integrals of the different signal patterns. Unfortunately, however, the resulting data reflect the sums of abundances of certain isotopologs (isotopolog sets) as opposed to the abundance of individual isotopologs. In order to establish a comprehensive description of the NMR data, we introduced a specialised nomenclature (Eisenreich et al., 2004) where the labelling pattern of any given glucose molecule is described in binary code by a six digit number and where the first digit signifies C-1, the second digit signifies C-2 of glucose etc. The presence of ^{12}C in any position is indicated by 0 (zero), the presence of ^{13}C is indicated by 1 (one), and X is used to signify either ^{12}C or ^{13}C (wild-card symbol). Using this notation, [1-$^{13}C_1$]glucose is denoted by {100000}, [2-$^{13}C_1$]glucose is denoted by {010000}, and universally ^{13}C-labelled glucose (i.e., [U-$^{13}C_6$]glucose) is denoted by {111111}.

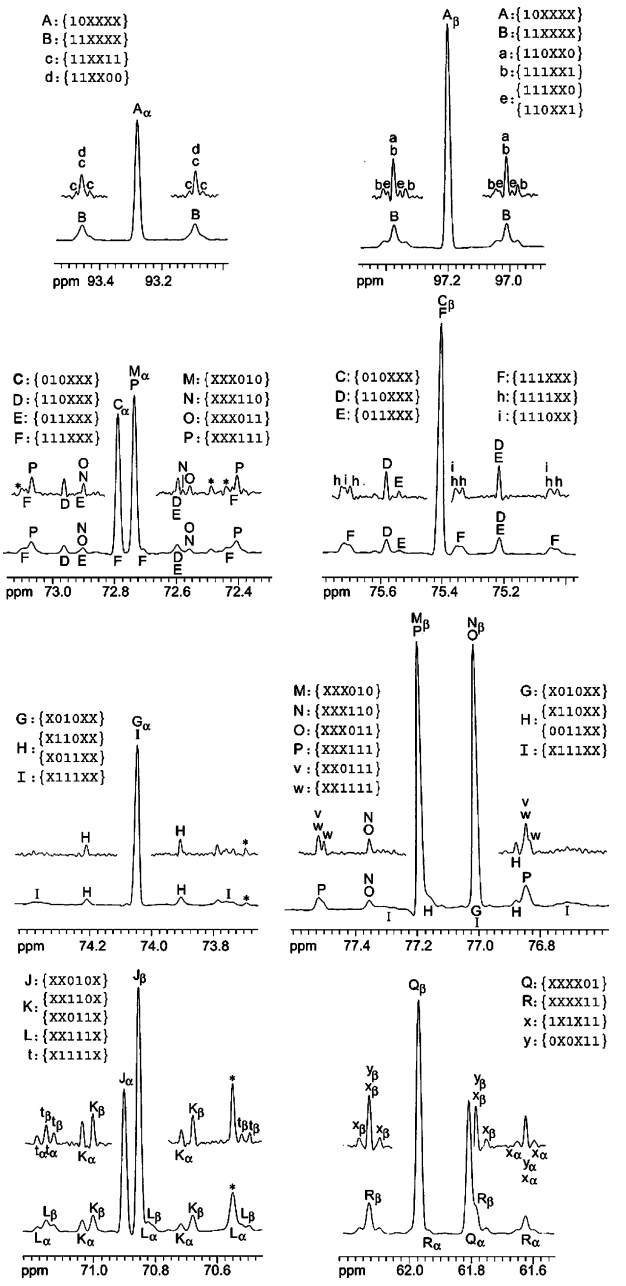

Fig. 2. ^{13}C NMR signals of glucose isolated from leaves of tobacco plants cultivated on a medium containing [U-$^{13}C_6$]glucose. The signals are assigned to corresponding X groups (cf. Tables 1–3). Asterisks indicate signals of contaminants.

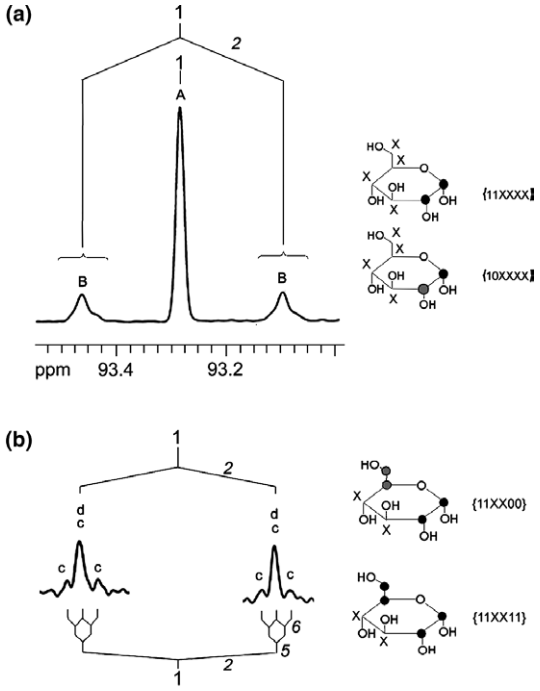

Fig. 3. ^{13}C NMR signal of C-1α of glucose isolated from tobacco cultivated on a medium containing [U-$^{13}C_6$]glucose. On the basis of known ^{13}C coupling constants, coupling patterns are indicated with the coupled atoms in italic letters. Next to the detected coupling patterns, the corresponding isotopolog groups are shown. Filled circles indicate ^{13}C and open circles ^{12}C, respectively. Undetermined positions (^{12}C or ^{13}C) are indicated by 'X'. Next to the structures, the corresponding X groups are given with 1 = ^{13}C, 0 = ^{12}C and X = ^{13}C or ^{12}C. A, spectrum calculated with a 'mild' Gaussian function; B, spectrum calculated with a 'strong' Gaussian function (only satellite signals are shown).

Using the wild-card denominator X, the set of isotopologs carrying ^{13}C in positions C-1 and C-2, ^{12}C in positions C-5 and C-6 and either ^{12}C or ^{13}C in any of the positions C-3 and C-4 can be denoted as {11XX00} reflected by the satellites indicated by d in Fig. 3; isotopolog sets of this type are subsequently designated X groups. On the basis of known ^{13}C coupling constants, specific spectral signatures can be assigned to the sum of abundances of the isotopologs which are members of a specific X group (for details, see Eisenreich et al., 2004). The assignment of specific signatures in the spectrum of glucose to the cognate X groups is summarised in Tables 1–3 and Fig. 2.

Since the X groups represent the sums of the concentrations of several different isotopologs, they are not easily interpreted in biochemical terms. It is therefore necessary to extract the concentrations of individual isotopologs from that data set. This is hampered by the fact that the present ^{13}C NMR spectrum allowed the determination of only 29 X groups (Table 3). On the other hand, we have to consider 64 individual isotopologs in glucose. Hence, the data set is markedly underdetermined and is not accessible to computational deconvolution.

That problem can be narrowed down to some extent by biochemical considerations. In the experiment under study, the amount of ^{13}C-labelled glucose is small by comparison with the total biomass of the tobacco plants. The cleavage of carbon bonds in the proffered ^{13}C-labelled glucose by catabolic processes affords smaller molecular species comprising a minimum number of one ^{13}C atom (in case that a single carbon fragment such as $^{13}CO_2$ is produced; larger cleavage products will contain more than one ^{13}C atom). The utilisation of these fragments as substrates for anabolic reactions can be conducive to the regeneration of glucose. However, on stochastic grounds, the molecular partners for such anabolic reactions will typically be derived from the unlabelled biomass of the plant (derived from unlabelled CO_2 and/or unlabelled sucrose in the medium), and their labelling patterns will therefore correspond to natural abundance. Hence, with very few exceptions, anabolic reactions will not be conducive to the connection of two different ^{13}C labelled fragments. Consequently, for the deconvolution of our experimental data, it is sufficient to consider glucose molecules carrying either uninterrupted blocks of ^{13}C atoms or single ^{13}C atoms. Obviously, it is then sufficient to consider one species with six ^{13}C atoms (i.e., the {111111} species), two molecular species with blocks of five uninterrupted ^{13}C atoms, three molecular species with blocks of four uninterrupted ^{13}C atoms, four molecular species with blocks of three uninterrupted ^{13}C atoms, five molecular species with blocks of 2 uninterrupted ^{13}C atoms, and finally six singly labelled glucose isotopologs. In summary, therefore, a total of 21 isotopologs needs to be determined. With this narrowed down requirement, the data set is overdetermined by the available 29 constraints and is now accessible to computational deconvolution.

Deconvolution was performed using a genetic algorithm that has been described elsewhere (Eisenreich et al., 2004). Specifically, deconvolution of the 29 X groups affords the abundances of 21 isotopologs with an average error of 0.02 mol% and a standard deviation of 0.03. The results are summarised in Figs. 4 and 5. It has to be emphasised that the determined isotopologs result from a temporal and spatial integration of the metabolic processes taking place in different tissues and compartments within the tobacco plant.

In the glucose isolated from tobacco leaves, the abundance of the singly labelled isotopologs is enhanced to approximately 1.62–1.83 mol% corresponding to ^{13}C excess of 0.52–0.73 mol%, respectively. The most abundant multiply labelled species is the {111111} isotopolog (0.39 mol%), i.e., the [U-$^{13}C_6$]glucose which had been proffered to the plants via the root system. Other multiply labelled species are the {000111} isotopolog (0.23 mol%), the {111000} isotopolog (0.16 mol%), the {000011} isotopolog (0.10 mol%) and the {110000} isotopolog (0.24 mol%). At lower abundance,

Table 1
NMR analysis of glucose (α-isomer) from *N. tabacum* grown on a medium with [U-$^{13}C_6$]glucose

Position	ppm	Signal[a]	X group[b]	Fraction in global signal, in %	Mol%
1α	93.280	A	10XXXX	69.5	1.67
	93.458, 93.094	B	11XXXX	30.5	0.73
	93.473, 93.458, 93.429, 93.109, 93.092, 93.067	c	11XX11	11.8	0.28
	93.458, 93.092	d	11XX00	18.7	0.45
2α	72.790	C	010XXX	80.3	1.93
	72.966, 72.598	D	110XXX	9.8	0.24
	72.914, 72.610	E	011XXX	1.9	0.05
	73.087, 72.790, 72.725, 72.417	F	111XXX	8.0	0.19
3α	74.050	G	X010XX	76.4	1.83
	74.210, 73.908	H	X110XX X011XX	8.2	0.20
	74.359, 74.050, 73.755	I	X111XX	15.4	0.37
4α	70.900	J	XX010X	68.2	1.64
	71.037, 70.717	K	XX110X XX011X	10.3	0.25
	71.165, 70.852, 70.548	L	XX111X	21.5	0.52
	71.183, 71.153, 70.852, 70.561, 70.532	t	X1111X	21.5	0.52
	71.165, 70.852, 70.548	u	X0111X	< 0.01	< 0.02
5α	72.737	M	XXX010	71.6	1.72
	72.905, 72.580	N	XXX110	1.0	0.02
	72.905, 72.560	O	XXX011	4.0	0.10
	73.070, 72.747, 72.405	P	XXX111	23.4	0.56
6α	61.812	Q	XXXX01	71.2	1.71
	61.970, 61.630	R	XXXX11	28.8	0.69
	62.000, 61.974, 61.940, 61.655, 61.630, 61.600	x	1X1X11	16.4	0.39
	61.970, 61.630	y	0X0X11	12.4	0.30

[a] Cf. signal labels in Figs. 2 and 3.
[b] 1 = ^{13}C; 0 = ^{12}C; X = ^{12}C or ^{13}C. For more details, see text.

but still above the detection limit, we observed the {011000}, {000110} and {001111} isotopologs (0.03, 0.02 and 0.01 mol%). No other multiply labelled isotopologs were observed in detectable amounts. However, it should be noted that the detection limit using NMR in the presented experimental setup is approximately 0.01 mol%.

Based on the molar excess of single and multiple labelled isotopologs, we simulated the data in silico by inference of the metabolic rules for circular processes (Table 4) implemented in the 4F software package (Ettenhuber and Eisenreich, 2004). An example of the method and the inference process is presented in Fig. 6. The deconvolution approach of the metabolic network operates rule-based as opposed to functional-based solutions (Gillespie, 1977; Schmidt et al., 1997; Wiechert et al., 1997; Wiechert and de Graaf, 1997; Follstadt and Stephanopoulos, 1998; Schmidt et al., 1998; Fiaux et al., 1999; Park et al., 1999; Wiechert et al., 1999; Wiechert and Murzel, 2001; van Winden et al., 2002). The software 4F was designed and implemented to solve exclusively circular metabolic networks which are difficult to model using conventional functional design strategies (for additional information on modelling and design strategies for complex systems, see Yourdon, 1989 and Powel-Douglass, 2004). Since tracer and 'tracee' (cf. Cobelli et al., 1992) are the same metabolite in the present study (i.e., glucose), no 'zero-fluxes' (cf. Roscher et al., 2000) were modelled in the system. The flux contributions obtained by in silico simulations for the intermediary metabolic processes (cf. Table 4) are summarised in Fig. 7. The simulated isotopolog excess deviates by less than 4.4% from the experimentally obtained isotopolog excess (cf. Table 5).

It can be concluded that the six metabolic processes implemented in the 4F software (i.e., glycolysis/glucogensis, transketolase and transaldolase reaction in the pentose phosphate cycle, citrate cycle, Calvin cycle, direct transfer of exogeneous glucose to leaf glucose) are sufficient to describe the key reactions involved in glucose metabolism of tobacco. The data show that the pentose phosphate cycle and the citrate cycle are the dominant processes in glucose recycling of the plant.

3. Discussion

There is widespread consensus about the requirement for a detailed analysis of metabolic networks in plants in the context of basic science as well as for practical

Table 2
NMR analysis of glucose (β-isomer) from *N. tabacum* grown on a medium with [U-$^{13}C_6$]glucose

Position	ppm	Signal[a]	X group[b]	Fraction in global signal, in %	Mol%
1β	97.200	A	10XXXX	69.0	1.67
	97.376, 97.012	B	11XXXX	30.6	0.73
	97.376, 97.012	a	110XX0	10.5	0.25
	97.409, 97.376, 97.337, 97.045, 97.010, 96.975	b	111XX1	16.2	0.39
	97.395, 97.356, 97.031, 96.992	e	111XX0 110XX1	4.7	0.11
2β	75.410	C	010XXX	67.5	1.62
	75.582, 75.217	D	110XXX	9.1	0.22
	75.540, 75.234	E	011XXX	1.7	0.04
	75.712, 75.41, 75.348, 75.041	F	111XXX	21.5	0.52
	75.723, 75.698, 75.410, 75.389, 75.359, 75.336, 75.051, 75.028	h	1111XX	15.2	0.36
	75.712, 75.410, 75.348, 75.041	i	1110XX	6.6	0.16
3β	77.090	G	X010XX	65.3	1.57
	77.160, 76.890	H	X110XX X011XX	19.5	0.47
	77.320, 77.090, 76.700	I	X111XX	15.2	0.36
4β	70.853	J	XX010X	69.0	1.65
	70.002, 70.678	K	XX110X XX011X	12.4	0.30
	71.142, 70.823, 70.502	L	XX111X	18.6	0.45
	71.153, 71.129, 70.823, 70.518, 70.494	t	X1111X	18.6	0.45
	71.143, 70.823, 70.506	u	X0111X	0.01	< 0.01
5β	77.190	M	XXX010	72.00	1.73
	77.350, 77.023	N	XXX110	3.61	0.09
	77.352, 77.012	O	XXX011		
	77.517, 77.190, 76.847	P	XXX111	24.39	0.59
	77.519, 77.501, 77.190, 76.847, 76.835	w	XX1111	15.1	0.36
	77.515, 77.190, 76.845	v	XX0111	9.3	0.23
6β	61.970	Q	XXXX01	70.7	1.70
	62.132, 61.787	R	XXXX11	29.3	0.70
	62.165, 62.132, 62.098, 61.815, 61.789, 61.756	x	1X1X11	14.5	0.35
	62.132, 61.787	y	0X0X11	14.8	0.36

[a] Cf. signal labels in Figs. 2 and 3.
[b] 1 = ^{13}C; 0 = ^{12}C; X = ^{12}C or ^{13}C. For more details, see text.

applications in plant breeding and crop production. Major progress has been made in the areas of transcriptional profiling, metabolic profiling and computational simulation (Bligny and Douce, 2001; Ratcliffe et al., 2001; Kruger et al., 2003; Fiaux et al., 1999; Gillespie and Petzold, 2004; Sriram and Shanks, 2004). Using advanced solid phase technology, it is now possible to simultaneously monitor the transcription of large numbers of genes with relatively little effort. Similarly, large numbers of metabolites can now be monitored quantitatively by mass spectrometry. Last not least, progress in computational sciences has enabled the simulation of complex multiparameter systems such as the dynamic interactions in multienzyme systems with an acceptable amount of computer time.

Without detracting from the impressive progress that has been made, it should be noted, however, that each of these methods is fraught with certain handicaps. The accuracy of RNA profiling in quantitative terms is limited, and the annotation of genomes is as yet incomplete and sometimes erroneous. More important, even if all messages were translated with the same efficacy, the precise functional status of each respective gene product in the system under study cannot be addressed with present-day technology.

Metabolite profiling can be performed with impressive accuracy but monitors only the net production or net consumption of metabolites and is unable to address the complexity of reversible processes in real world metabolic systems. Finally, computer simulations are hampered by the precision of available models and parameters; to begin with, the kinetic models used for enzymes are at best approximations, and the accuracy of literature data on kinetic properties of enzymes is fairly limited. Last not least, the topological complexity of plants and plant cells and the role of diffusion barriers in that small-scale world appears difficult to be modelled in realistic ways.

The isotopolog perturbation/relaxation technology described in this paper has the potential to complement

Table 3
Molar abundances of isotopomer sets in glucose from *N. tabacum* in the experiment with [U-$^{13}C_6$]glucose

X group	Signal[a]	Molar abundance (mol %)		
		α-Glucose	β-Glucose	Average
10XXXX	A	1.67	1.67	**1.670**
11XXXX	B	0.73	0.73	**0.730**
110XX0	a		**0.25**	
111XX1	b		**0.39**	
11XX11	c	**0.28**		
11XX00	d	**0.45**		
111XX0	e		**0.11**	
010XXX	C	nd	**1.62**	
110XXX	D	nd	**0.22**	
011XXX	E	nd	**0.04**	
111XXX	F	nd	**0.52**	
1111XX	h	nd	**0.36**	
1110XX	i	nd	**0.16**	
X010XX	G	**1.83**	nd	
X110XX	H	**0.20**	nd	
X011XX				
X111XX	I	**0.37**	nd	
XX010X	J	1.64	1.65	**1.645**
XX110X		0.25	0.30	**0.275**
XX011X	K			
XX111X	L	0.52	0.45	**0.485**
XXX010	M	1.72	1.73	**1.725**
XXX110	N	**0.02**	0.09	
XXX011	O	**0.10**		
XXX111	P	0.56	0.59	**0.575**
XXXX01	Q	1.71	1.70	**1.705**
XXXX11	R	0.69	0.70	**0.695**
1X1X11	x	**0.39**	nd	
0X0X11	y	**0.30**	nd	

Molar abundances in bold-type printing were used as input for the deconvolution algorithm.
[a] Cf. signal labels in Figs. 2 and 3.

the methods listed above and to address some of their shortcomings. Most notably, it can be used to dissect reversible processes which are typical for complex metabolic systems. Notably, the method is not in any way limited to the use of glucose as perturbant and/or analyte. On the contrary, any compound or compound mixture that can be absorbed and metabolised by the biological system under study can be proffered in selectively or universally isotope-labelled form, and any metabolite that can be isolated in sufficient amounts to allow isotopolog analysis can be used for evaluation. Most notably, multiple analytes can be processed in a given experiment.

The present work shows that metabolism in tobacco and probably other green plants grown on agar can be studied on a quantitative basis with a mixture of sucrose and ^{13}C-labelled glucose added to the agar. The labelled glucose is efficiently absorbed via the root system and metabolised. It is also obvious that the carbohydrate is efficiently recycled in tobacco plants.

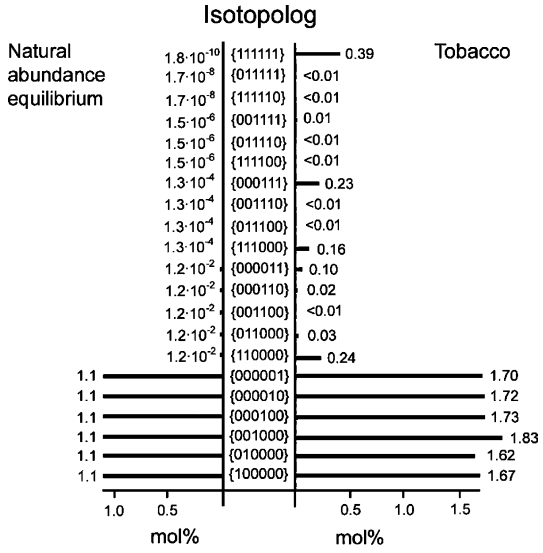

Fig. 4. Natural ^{13}C abundance of selected glucose isotopologs versus their abundance in glucose from tobacco leaves in the experiment with [U-$^{13}C_6$]glucose.

In the group of the detected ^{13}C enriched isotopologs of glucose (single and multiple labelled species; total amount of ^{13}C excess (T) equals 4.85 mol%, cf. Fig. 5) 0.39 mol% are found as the {111111} isotopolog. In other words, 8% of the labelled glucose isolated from the leaves have retained the bond connectivity of [U-$^{13}C_6$]glucose that was proffered via the root system; 92% have been broken into pieces and reassembled at least once by metabolic processes outlined below.

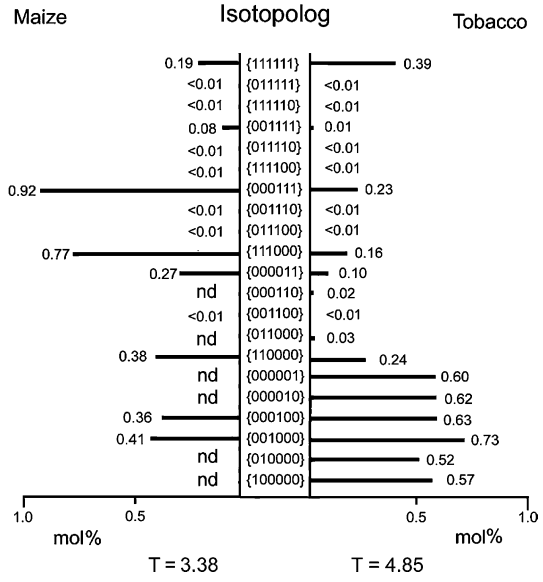

Fig. 5. ^{13}C excess in experiments with kernels of *Zea mays* (Glawischnig et al., 2002) and growing plants of *N. tabacum* (this study) using [U-$^{13}C_6$]glucose as perturbant. It should be noted that this figure shows isotopolog excess whereas Fig. 4 shows isotopolog abundance.

Table 4
Metabolic transfer rules implemented in the 4F software (Ettenhuber and Eisenreich, 2004) used to simulate isotopolog compositions in experiments using [U-$^{13}C_6$]glucose as tracer analyte

Rule	Operation
"emp"	Cycling via glycolysis/glucogenesis or pentose phosphate cycle from glucose 6-phosphate to triose phosphate and reverse. The first part of the rule 'emp' formalizes the cleavage and regeneration of glucose. The second part of the rule 'emp' formalizes the possible interchange of the triose moieties. emp1: $\{XXXXXX\} \rightarrow \{XXX000\} + \{000XXX\}$ emp2: $\{XXX000\} + \{000XXX\} \rightarrow \{XXX000\} + \{000XXX\}$
"tk"	Cycling via the transketolase reaction of the pentose phosphate pathway. tk1: $\{XXXXXX\} \rightarrow \{XX0000\} + \{00XXXX\}$
"ta"	Glycerinaldehyde 3-phosphate and sedoheptulose 7-phosphate yield an asymmetric isotopolog distribution in catabolic processes. The resulting fructose 6-phosphate connects glycolysis and transaldolase reaction in the non-oxidative branch of the pentose phosphate pathway. ta1: $\{XXXXXX\} \rightarrow \{000XXX\}$
"dtr"	Transfer of exogeneous glucose into leaf glucose without further metabolic cycling events. dtr1: $\{XXXXXX\} \rightarrow \{XXXXXX\} \mid \forall X = 1$
"tca"	Glucogenesis via oxaloacetate in the citric acid cycle. tca1: $\{XXXXXX\} \rightarrow \{X00000\} + \{0XX000\} + \{000XX0\} + \{00000X\}$
"cof"	$^{13}CO_2$ refixation yields labelled [3-$^{13}C_1$]phosphoglycerate through the Calvin cycle. The $^{13}CO_2$ can be generated from any position of the proffered ^{13}C-labelled glucose. cof1: $\{XXXXXX\} \rightarrow \{00X000\} + \{000X00\}$

For a detailed description of the X group nomenclature, see text.

The relatively high abundance of the {111000} and the {000111} isotopologs is explained by the operation of glycolysis followed by glucogenesis (Fig. 8A). However, both isotopologs can also be formed by grafting unlabelled three carbon blocks to 3-carbon moieties derived from the labelled precursor by the catalytic action of the transaldolase.

The formation of the {001111} isotopolog (0.01 mol%) can be explained as a result of the action of transketolase transferring a two-carbon fragment from labelled ketulose phosphate to $^{13}C_4$ tetrose phosphate derived from [U-$^{13}C_6$]fructose 6-phosphate (Fig. 8B). The question why we observed a much higher level of a corresponding {110000} isotopolog will be addressed later.

The glycolytic pathway as well as the action of transaldolase result in the cleavage of the bond between C-3 and C-4 of glucose. The low abundance (0.01 mol%) of the {001111} glucose isotopolog that one would expect to be formed by the operation of the transketolase reaction in the pentose phosphate cycle (as opposed to 0.24

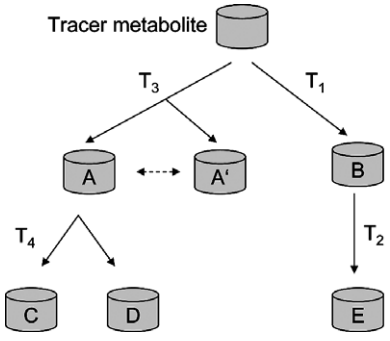

Fig. 6. Example for the 4F algorithm of the feed forward flux estimation algorithm which is able to simulate metabolic circuits. It can be applied for experimental setups in which tracer and analyte molecule are isotopologs of the same compound. Assume that a pool of the tracer metabolite can be transformed by the metabolic operations T_1, T_2, T_3 and T_4. T_3 is defined by a symmetric operation for the given example. In the forward flux phase, T_3 and T_1 fill A, A′ and B. T_4 generates from A the isotopologs C and D. C and D are filled until they are equilibrated or A is depleted. In either case a slipstream from the tracer pool and balancing between A and A′ must occur in the counterflux phase. The same holds true for B and E. The filling of E depletes B. Thus a slipstream from the tracer pool must occur until B and E are balanced with the experimentally obtained constraints.

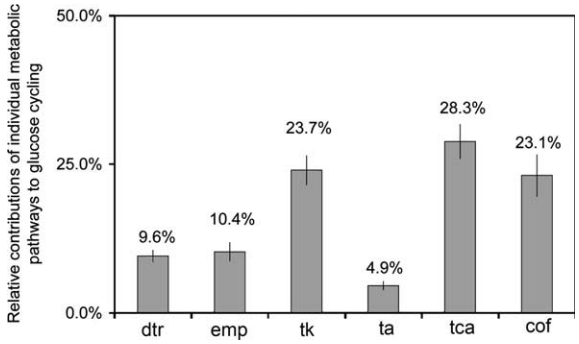

Fig. 7. Flux contributions of central metabolic processes in glucose recycling of tobacco. The relative fluxes were simulated by the 4F algorithm (Ettenhuber and Eisenreich, 2004). The direct transfer of intact exogeneous glucose to leaf glucose ("dtr"), glycolysis/glucogenesis reaction ("emp"), transketolase reaction of the pentose phosphate pathway ("tk"), transaldolase reaction of the pentose phosphate pathway ("ta"), the Krebs cycle through regeneration of glucose via oxaloacetate ("tca"), and the refixation of $^{13}CO_2$ via the Calvin cycle ("cof").

Table 5
Comparison of spectroscopically observed ^{13}C excess (in mol %) of glucose isotopologs from tobacco leaves in the experiment with [U-$^{13}C_6$]glucose with the 4F simulated ^{13}C excess using the transfer rules given in Table 4.

Glucose isotopolog	Experimental ^{13}C excess	Simulated ^{13}C excess
{100000}	0.57	0.57
{010000}	0.52	0.50
{001000}	0.73	0.73
{000100}	0.62	0.60
{000010}	0.62	0.60
{000001}	0.60	0.57
{110000}	0.24	0.24
{011000}	0.02	0.02
{000110}	0.03	0.03
{000011}	0.10	0.10
{111000}	0.16	0.09
{000111}	0.23	0.23
{001111}	0.01	0.02
{111111}	0.39	0.39

mol% of the orthogonal {110000} isotopolog) suggests that consecutive metabolic cycles using the {001111} isotopolog as starting material occur with considerable frequency (Fig. 8B).

The formation of the {000011} isotopolog could be due to second cycle processes starting with the relatively abundant {110000} isotopolog that has been described above. Glycolytic cleavage of that species followed by rapid isomerisation of the resulting triose phosphate by triose phosphate isomerase could afford [2,3-$^{13}C_2$]glyceraldehyde 3-phosphate which could then be converted to the {000011} glucose species by the action of the glucogenetic pathway or, alternatively, by the action of transaldolase (see Fig. 9).

The {011000} isotopolog carrying a block of two ^{13}C atoms must be assumed to have been formed by a relatively complex sequence of events because at least two carbon carbon bonds of the original, universally ^{13}C-labelled glucose must have been broken in the process (Fig. 8C). More specifically, this isotopolog could arise by decarboxylation of pyruvate (resulting from glycolytic cleavage of universally labelled glucose) affording [1,2-$^{13}C_2$]acetyl-CoA which could then be processed by the citrate cycle affording [1,2-$^{13}C_2$]oxaloacetate. This may be converted into [1,2-$^{13}C_2$]phosphoenolpyruvate which may further be converted into [1,2-$^{13}C_2$]glyeraldehyde 3-phosphate and [1,2-$^{13}C_2$]dihydroxyacetone 3-phosphate. Ultimately, glucogenesis involving these double-labelled molecules could explain the formation of the {011000} and {000110} species which are present at almost equal abundances.

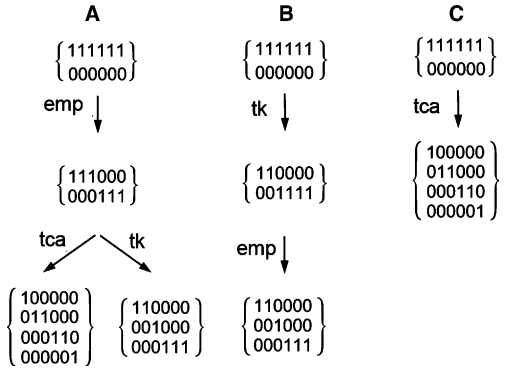

Fig. 8. Hierarchy of isotopolog groups originating by "emp", "tk" and "tca". Transformations leading to identical sets are not shown. All transformation become an identity transformation in repetitive application. The order of the transformations is indifferent as shown by the combination of "tk" and "emp" in A and B.

The large excess of $^{13}C_1$-labelled isotopologs in leaf glucose (cf. Fig. 5) can be explained by multiple cycling and refixation of $^{13}CO_2$ through the Calvin cycle. Not unexpectedly, this group constitutes the largest fraction of leaf glucose in the long-term experiment. For example, the isotopolog species {100000} and {000001} can arise from the citric acid cycle (cf. Eisenreich et al., 2004) or from fully or partially labelled glucoses. {010000}, {000010}, {001000}, and {000100} can arise by cleavage of {011000} and {000110} from the citric acid cycle in a second cycle *via* the transketolase reaction. The {001000} and {000100} isotopologs can also be obtained by fixation of $^{13}CO_2$ in the Calvin cycle.

The formal analysis of the observed ^{13}C isotopologs including the data simulation using the rule-based 4F software (Ettenhuber and Eisenreich, 2004) shows that extensive cycling of labelled glucose molecules takes place in the plant system. The in silico simulation afforded relative contributions of the metabolic processes involved in this recycling process. Thus cycling via the pentose phosphate pathway and citrate cycle were the dominant processes with 28.6% and 28.3%, respectively, of all metabolic events (Fig. 7). This is particularly reflected by the high ^{13}C excess of the corresponding single-labelled isotopolog species. Refixation of $^{13}CO_2$ takes place at significant rates, since 23.1% of the total cycling events are represented by the Calvin cycle (Fig. 7). Fragmentation through glycolysis/glucogenesis occured at lower frequency (10.3% of total metabolic cycling).

It is obvious that all proffered glucose molecules that have been metabolically fragmented with consecutive regeneration of multiply ^{13}C-labelled glucose species must have entered at least one plant cell type prior to their reisolation. It is as yet unknown whether this cycling happens already in the root system or later in the leaves; quite probably, various tissues contribute to the results of our perturbation/relaxation experiment. Obviously, the glucose molecules in question must then have been phosphorylated, and ultimately glucose must have been regenerated by dephosphorylation. As for the {111111} molecules, it remains unknown whether they have undergone a phosphorylation/dephosphorylation

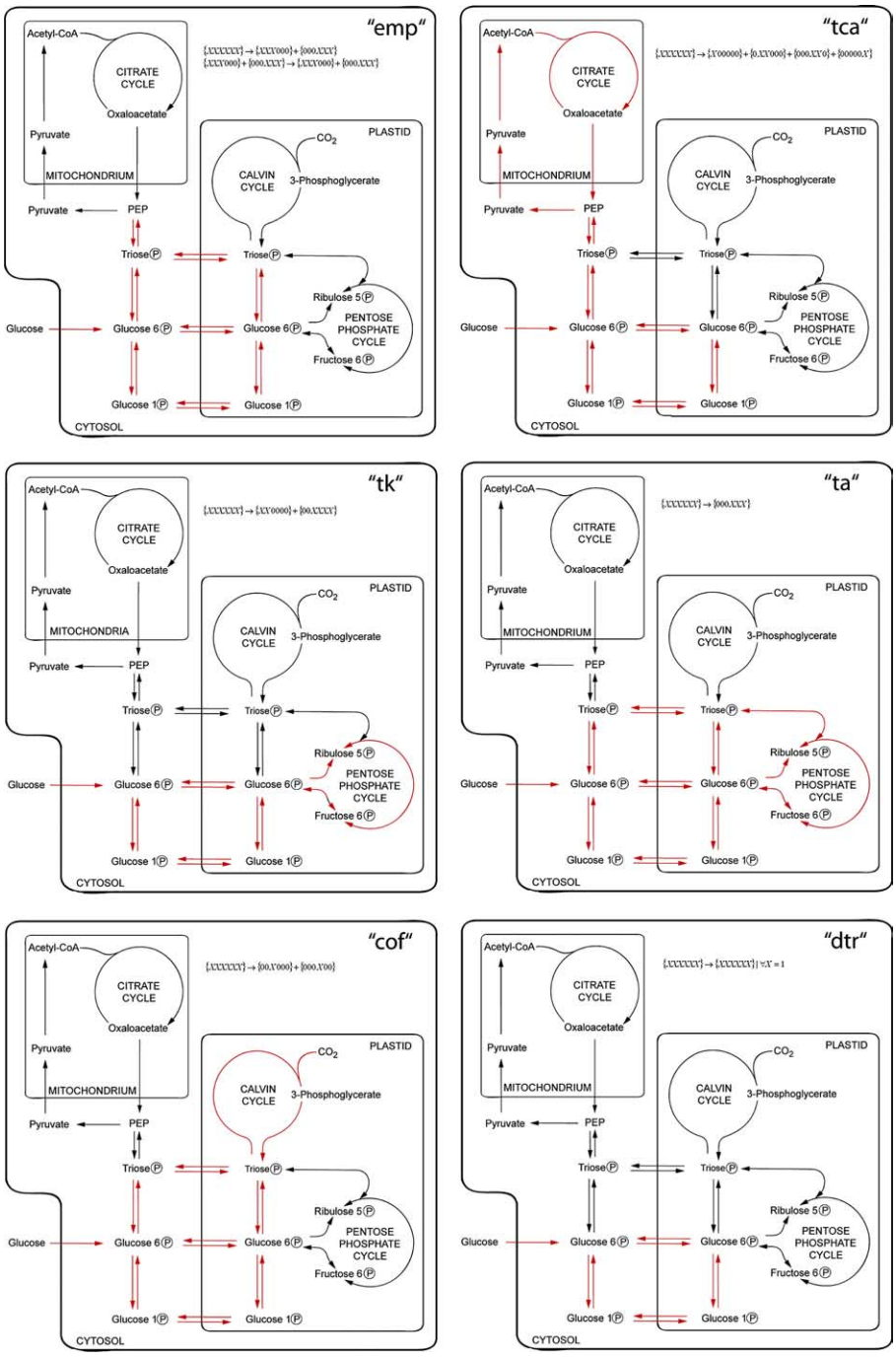

Fig. 9. Metabolic network involved in the formation of multiple ^{13}C labelled isotopologs of glucose in plants of *N. tabacum* grown with [U-$^{13}C_6$]glucose. Simulated circular pathways are shown in red. The transfer rules correspond to the single metabolic circuits and formalize the change of the glucose isotopolog signature (for detailed information on the rules, see Table 4).

cycle without further metabolisation or whether they have been exclusively transported in extracellular fluids.

In a different experimental setup, we had shown earlier that glucose molecules are rapidly disassembled/reassembled prior to the incorporation into starch by maize kernels in tissue culture which is devoid of photosynthetic activity (Glawischnig et al., 2002). Although that experiment utilised a much simpler technology for analysis of isotopolog patterns, the data allow certain valid comparisons.

In the earlier experiment with maize kernels, the multiply labelled isotopolog population was dominated by the two triple-labelled species, {111000} and {000111} (cf. Fig. 5). As mentioned above, these two isotopologs both result from breakdown of proffered glucose to triose phosphate followed by glucogenesis. Hence, we con-

clude that glycolysis/glucogenesis and/or the transaldolase reaction of the pentose phosphate cycle plays a much larger role in the reshaping of glucose in the maize experiment as compared to the tobacco experiment. Since the tobacco experiments were performed under long day illumination conditions and involved net fixation of CO_2, the plastid-based Calvin cycle played an important role in the scrambling of label. On the other hand, the maize experiments did not involve photosynthesis. These findings show that the perturbation/relaxation experiment with [U-$^{13}C_6$]glucose as tracer is well qualified to distinguish between different metabolic situations in plant cells.

In order to appreciate the specific role of the Calvin cycle in the tobacco plants, it should be mentioned that both the illumination and the supply of CO_2 were not sufficient to support growth, and plants were predominantly relying on the proffered carbohydrates for growth and metabolism. It must further be considered that the photosynthetic activity was further depressed by catabolite repression caused by the ample supply of exogenous carbohydrates. The experimental method described in this paper appears to be ideally suited to study these factors in more detail.

It should also be emphasised that the methodology is not restricted to tobacco plants. On the contrary, the study appears to be a valid model for metabolic flux analysis of plants in general provided that the plant under study can be grown on agar. Under these circumstances, the system appears to be well qualified to study flux contributions in the biosynthesis of sink metabolites, such as carbohydrates, organic acids or secondary metabolites.

4. Experimental

4.1. Materials

[U-$^{13}C_6$]Glucose (99% ^{13}C abundance) was purchased from Isotec (Miamisburg, OH).

4.2. Plants

Tobacco plants (*Nicotiana tabacum* L, cv. Petite Havana) were grown under aseptic conditions from sterilised seeds or shoot cutting explanted on B5 medium (Manandhar and Gresshoff, 1980) containing 2% (w/v) sucrose and solidified with 0.7% bacteriological agar. For isotope incorporation studies, the culture medium contained 400 mg of [U-$^{13}C_6$]glucose (99% ^{13}C abundance) and 19.8 g of unlabelled sucrose per litre.The plants were grown at 25 °C with 8/16 h dark/light illumination cycles at a light intensity of 0.5–1 W m^{-2} (Osram L85W/25 Universal White fluorescent lamps).

4.3. Isolation of glucose

Tobacco leaves (15 g wet weight) were harvested after a growth period of 20 days. They were frozen with liquid nitrogen, pulverised and extracted with water. The mixture was centrifuged, and the supernatant was lyophilised. The residue was dissolved in 3 ml of water. Aliquots were applied to a Rezex RNM-Carbohydrate HPLC column (Phenomenex, Torrance CA, USA) which was developed with water at 75 °C and a flow rate of 0.7 ml/min. The effluent was monitored refractometrically using a GAT LCD 201 differential refractometer from Gamma Analysen Technik GmbH, Bremerhaven, Germany. The retention volume of glucose was 14 ml. Fractions were combined and lyophilised.

4.4. NMR spectroscopy

Glucose was dissolved in 0.5 ml of D_2O. ^1H and ^{13}C NMR spectra were recorded at 500.13 and 125.76 MHz, respectively, using a Bruker DRX500 spectrometer, at 27 °C. Water suppression was achieved by presaturation of the residual water signal at the lowest possible power level. For ^1H-decoupling, a composite pulse sequence (WALTZ) was used in the ^{13}C NMR experiments. 30° pulses were applied with a repetition rate of 3.5 s. The data were processed with standard Bruker software (XWINNMR 3.0). Prior to Fourier transformation, the FID was zero-filled to 256k and multiplied with Gaussian functions. Typical parameters were −1 to −2 for lb and 0.1 to 0.4 for gb, respectively. Prior to integration, the baseline of the spectra was corrected.

The signal assignments, ^{13}C–^{13}C coupling constants, and isotope shifts of α- and β-glucose were published earlier (Eisenreich et al., 2004). The analysis of ^{13}C enrichment and isotopolog composition was performed as described (Eisenreich et al., 2004). Briefly, absolute ^{13}C abundance for C-1 was obtained from ^{13}C coupling satellites of H-1α (5.26 ppm) in the ^1H NMR spectrum. This value was taken as a reference for the ^{13}C abundances of the other carbon atoms.

In the ^1H-decoupled ^{13}C NMR spectrum, each signal was integrated separately. The relative fractions of each respective satellite pair (corresponding to a given coupling pattern, Tables 1 and 2) in the total signal integral of a given carbon atom were calculated. These values were then referenced to the global absolute ^{13}C abundance for each carbon atom (mol% in Table 3).

4.5. Data evaluation

The molar abundances of certain sets of isotopologs designated as X groups (see below) were determined as described earlier (Eisenreich et al., 2004). The abundances

of individual isotopologs were then obtained by computational deconvolution of X group abundance using a genetic algorithm (Holland, 1975; Rechenberg, 1973) implemented by the GeneHunter library (WardSystems Inc., Frederick, MD). A detailed description of the methods used is given in Eisenreich et al. (2004).

Isotopolog excess was assigned to fractions of metabolic processes involved in the glucose cycling in the kernel system. The applied algorithm (which we designate as 4F algorithm) is implemented as. NET software service (Ettenhuber and Eisenreich, 2004). The program simulates the molar excess of individual ^{13}C-labeled isotopologs from a pool of [U-$^{13}C_6$]glucose and glucose with natural abundance by inference of the rules given in Table 4. Specifically, glycolytic cycling via glycolysis (''emp''), the transketolase reaction of the pentose phosphate pathway (''tk''), the transaldolase reaction of the pentose phosphate pathway (''ta''), the citrate cycle (''tca''), the refixation of $^{13}CO_2$ (''cof'') and the direct transport of glucose to leaf tissue (''dtr'') are implemented in the program. The rules are not commutative and are executed according to their priority. Metabolic processes yielding asymmetric isotopologs have higher priority than processes yielding symmetric isotopologs. The more isotopologs are generated by applying a rule, the higher is the priority of this rule. For the given metabolic topology, the priority of the rules in ascending order is ''dtr'', ''ta'',''cof'', ''emp'', ''tk'', ''tca''.

For the simulation, a bottom-up approach is used. Isotopologs derived from multiple cycling events are generated by a forward feeding phase, while isotopologs derived from single transformations are generated by the subsequent slipstreams. According to this rule, excess of isotopologs having the most complex biosynthetic history (i.e., with multiple cycling events) are generated first by direct forward feeding of glucose from the [U-$^{13}C_6$]glucose pool to the network via pools of multiple-labelled glucose isotopologs. Slipstreams from the [U-$^{13}C_6$]glucose pool are subsequently used to refill ^{13}C excess from isotopologs with a lower metabolic complexity. Symmetric isotopologs derived from single metabolic operations are then balanced according to asymmetric transfer reactions. The algorithm works iteratively until the tracer pool is depleted or the similarity between simulated and experimental glucose isotopolog values cannot be improved further. The amount of glucose transformed by execution of a single rule is defined by an application specific iterator size (in this case 0.001 mol%). An example of the execution of the algorithm is shown in Fig. 6. The output of this iteration reveals the fraction of specific cycling events (i.e., assigned to individual circular pathways).

Errors of the NMR experiment are propagated via the glucose isotopolog abundances to the fraction of the executed rules in two steps: (I) For each X group an estimated experimental error of 10% is propagated via the final X group state matrix (described in Eisenreich et al., 2004) to the single glucose isotopologs. (II) Metabolic rules are related to isotopologs by metabolic transfer rules (Table 4) and the error deviation of each isotopolog can therefore be propagated to the relative fraction of a specific circular pathway in the simulation.

Acknowledgments

This work was supported by grants from the Deutsche Forschungsgemeinschaft, the Fonds der Chemischen Industrie and the Hans Fischer Gesellschaft. We thank Fritz Wendling and Christine Schwarz for expert technical assistance.

References

Arabidopsis Genome Initiative, 2001. Analysis of the genome sequence of the flowering plant *Arabidopsis thaliana*. Nature 408, 796–815.

Bacher, A., Rieder, C., Eichinger, D., Fuchs, G., Arigoni, D., Eisenreich, W., 1999. Elucidation of biosynthetic pathways and metabolic flux patterns via retrobiosynthetic NMR analysis. FEMS Microbiol. Rev. 22, 567–598.

Bligny, R., Douce, R., 2001. NMR and plant metabolism. Curr. Opin. Plant. Biol. 4, 191–196.

Bray, D., 2003. Molecular networks: the top-down view. Science 301, 1864–1866.

Brunengraber, H., Kelleher, J.K., Des Rosiers, C., 1997. Applications of mass isotopomer analysis to nutrition research. Annu. Rev. Nutr. 17, 559–596.

Clifton, S.W., Roe, B.A., 1998. The beautifully simple but intriguingly complex world of small genomes. Genome Res. 8, 331–333.

Cobelli, C., Toffolo, G., Foster, D.M., 1992. Tracer-to-tracee ratio for analysis of stable isotope tracer data: link with radioactive kinetic formalism. Am. J. Physiol. 262, 968–975.

Eisenberg, D., Marcotte, E.M., Xenarios, I., Yeates, T.O., 2000. Protein function in the post-genomic era. Nature 405, 823–826.

Eisenreich, W., Ettenhuber, C., Laupitz, R., Theus, C., Bacher, A., 2004. Isotopolog perturbation techniques for metabolic networks: Metabolic recycling of nutritional glucose in *Drosophila melanogaster*. Proc. Natl. Acad. Sci. USA 101, 6764–6769.

Eisenreich, W., Strauß, G., Werz, U., Bacher, A., Fuchs, G., 1993. Retrobiosynthetic analysis of 1 carbon fixation in the phototrophic eubacterium *Chloroflexus aurantiacus*. Eur. J. Biochem. 215, 619–632.

Ettenhuber, C., Eisenreich, W., 2004. 4F service 1.0. Available from: http://xsystem.org.chemie.tu-muenchen.de.

Fey, S.J., Nawrocki, A., Larsen, M.R., Gorg, A., Roepstorff, P., Skews, G.N., Williams, R., Larsen, P.M., 1997. Proteome analysis of *Saccharomyces cerevisiae*: a methodological outline. Electrophoresis 18, 1361–1372.

Fiaux, J., Andersson, C.J.Y., Holmberg, N., Bülow, L., Kallio, P.T., Szyperski, T., Bailey, J.E., Wüthrich, K., 1999. ^{13}C NMR flux ratio analysis of *Escherichia coli* central carbon metabolism in microaerobic bioprocesses. J. Am. Chem. Soc. 121, 1407–1408.

Fiehn, O., Kopka, J., Dormann, P., Altmann, T., Trethewey, R.N., Willmitzer, L., 2000. Metabolite profiling for plant functional genomics. Nat. Biotechnol. 18, 1157–1161.

Follstadt, B.D., Stephanopoulos, G., 1998. Effect of reversible reaction on isotope label redistribution. Analysis of the pentose phosphate pathway. Eur. J. Biochem. 202, 360–371.

Fraser, C.M. et al., 1995. The minimal gene complement of *Mycoplasma genitalium*. Science 270, 397–403.

Gillespie, D.T., 1977. Exact stochastic simulation of coupled chemical reactions. J. Phys. Chem. 81, 2340–2361.

Gillespie, D.T., Petzold, L.R., 2004. Improved leap-size selection for accelerated stochastic simulation. J. Chem. Phys. 119, 8229–8234.

Glawischnig, E., Gierl, A., Tomas, A., Bacher, A., Eisenreich, W., 2002. Retrobiosynthetic nuclear magnetic resonance analysis of amino acid biosynthesis and intermediary metabolism. Metabolic flux in developing maize kernels. Plant Physiol. 130, 1717–1727.

Gleixner, G., Daniel, H.J., Werner, R.A., Schmidt, H.L., 1993. Correlations between the ^{13}C content of primary and secondary plant products in different cell compartments and that in decomposing Basidiomycetes. Plant Physiol. 4, 1287–1290.

Goff, S.A. et al., 2002. A draft sequence of the rice genome (*Oryza sativa* L. ssp. *japonica*). Science 296, 92–100.

Holland, J.H., 1975. Adaptation in natural and artificial systems. Ph.D. Thesis, University of Michigan.

International Human Genome Sequencing Consortium, 2004. Finishing the euchromatic sequence of the human genome. Nature 431, 931–945.

Kruger, N.J., Ratcliffe, R.G., Roscher, A., 2003. Quantitative approaches for analysing fluxes through plant metabolic networks using NMR and stable isotope labelling. Phytochem. Rev. 2, 17–30.

Lockhart, D.J., Winzeler, E.A., 2000. Genomics, gene expression and DNA arrays. Nature 405, 827–836.

Manandhar, A., Gresshoff, P.M., 1980. Blue spruce (*Picea pungens*) tissue and cell culture. Cytobiosphere 29, 175–182.

Müller, W., Fricke, H., Halliday, A.N., McCulloch, M.T., Wartho, J.A., 2003. Origin and migration of the Alpine Iceman. Science 203, 862–866.

Park, S.M., Klapa, M.I., Sinskey, A.J., Stephanopoulos, G., 1999. Metabolite and isotopomer balancing in the analysis of metabolic cycles: II. Appl. Biotechnol. Bioeng. 62, 392–401.

Powel-Douglass, B., 2004. Real Time UML, third ed. Addison-Wesley.

Ratcliffe, R.G., Roscher, A., Shachar-Hill, Y., 2001. Plant NMR spectroscopy. Prog. Nucl. Magn. Reson. Spectrosc. 39, 267–300.

Rechenberg, I., 1973. Evolution strategies. Ph.D. Thesis, University of Stuttgart.

Rice Chromosome 10 Sequencing Consortium, 2003. In-depth view of structure, activity, and evolution of rice chromosome 10. Science 300, 1566–1569.

Roscher, A., Kruger, N.J., Ratcliffe, R.G., 2000. Strategies for metabolic flux analysis in plants using isotope labelling. J. Biotechnol. 77, 81–102.

Rossmann, A., Butzenlechner, M., Schmidt, H.L., 1991. Evidence for a nonstatistical carbon isotope distribution in natural glucose. Plant Physiol. 96, 609–614.

Schmidt, H.L., 2003. Fundamentals and systematics of the nonstatistical distributions of isotopes in natural compounds. Naturwissenschaften 90, 537–552.

Schmidt, K., Carlsen, M., Nielsen, J., Villadsen, J., 1997. Modeling isotopomer distributions in biochemical networks using isotopomer mapping matrices. Biotechnol. Bioeng. 55, 831–840.

Schmidt, K., Marx, A., de Graaf, A.A., Wiechert, W., Sahm, H., Nielsen, J., Villadsen, J., 1998. ^{13}C Tracer experiments and metabolite balancing for metabolic flux analysis: comparing two approaches. Biotechnol. Bioeng. 58, 254–257.

Sriram, G., Shanks, J.V., 2004. Improvements in metabolic flux analysis using carbon bond labeling experiments: bondomer balancing and Boolean function mapping. Metab. Eng. 6, 116–132.

Szyperski, T., 1995. Biosynthetically directed fractional ^{13}C-labeling of proteinogenic amino acids. An efficient analytical tool to investigate intermediary metabolism. Eur. J. Biochem. 232, 433–438.

van Winden, W., Heijnen, J.J., Verheijen, P.J.T., 2002. Cumulative bondomers: a new concept in flux analysis from 2D ^{13}C, 1H COSY NMR data. Biotechn. Bioeng. 80, 731–745.

Wiechert, W., Möllney, M., Isermann, N., Murzel, M., de Graaf, A.A., 1999. Bidirectional reaction steps in metabolic networks: III. Explicit solution and analysis of isotopomer labeling systems. Biotechnol. Bioeng. 66, 69–85.

Wiechert, W., Murzel, M., 2001. Metabolic isotopomer labeling systems. Part I: global dynamic behaviour. Math. Biosci. 169, 173–205.

Wiechert, W., de Graaf, A.A., 1997. Bidirectional reaction steps in metabolic networks: I. Modeling and simulation of carbon isotope labeling experiments. Biotechnol. Bioeng. 55, 101–117.

Wiechert, W., Siefke, C., de Graaf, A.A., Marx, A., 1997. Bidirectional reaction steps in metabolic networks: II. Flux estimation and statistical analysis. Biotechnol. Bioeng. 55, 118–135.

Yamada, K., Lim, J., Dale, J.M., Chen, H., Shinn, P., Palm, C.J., Southwick, A.M., Wu, H.C., Kim, C., Nguyen, M., Pham, P., Cheuk, R., Karlin-Newmann, G., Liu, S.X., Lam, B., Sakano, H., Wu, T., Yu, G., Miranda, M., Quach, H.L., Tripp, M., Chang, C.H., Lee, J.M., Toriumi, M., Chan, M.M., Tang, C.C., Onodera, C.S., Deng, J.M., Akiyama, K., Ansari, Y., Arakawa, T., Banh, J., Banno, F., Bowser, L., Brooks, S., Carninci, P., Chao, Q., Choy, N., Enju, A., Goldsmith, A.D., Gurjal, M., Hansen, N.F., Hayashizaki, Y., Johnson-Hopson, C., Hsuan, V.W., Iida, K., Karnes, M., Khan, S., Koesema, E., Ishida, J., Jiang, P.X., Jones, T., Kawai, J., Kamiya, A., Meyers, C., Nakajima, M., Narusaka, M., Seki, M., Sakurai, T., Satou, M., Tamse, R., Vaysberg, M., Wallender, E.K., Wong, C., Yamamura, Y., Yuan, S., Shinozaki, K., Davis, R.W., Theologis, A., Ecker, J.R., 2003. Empirical analysis of transcriptional activity in the *Arabidopsis* genome. Science 302, 842–846.

Yourdon, E., 1989. Modern Structured Systems Analysis. Prentice-Hall, Englewood Cliffs, NJ.